

DEPARTMENT OF CHEMISTRY

Design and Synthesis of Novel Fosmidomycin Analogues as Bisubstrate Dxr Inhibitors to Combat Malaria and Tuberculosis

G. Logan Bartholomew¹, Kenneth M. Heidel¹, Richard V. Beck¹, Rachel L. Edwards², Dana M. Hodge³, Haley Ball⁴, Audrey R. Odom John³, Robin D. Couch⁴, Cynthia S. Dowd¹

¹The Department of Chemistry, The George Washington University, Washington, DC

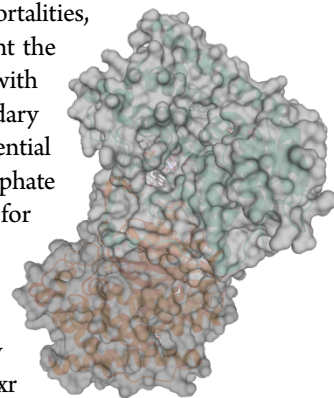
²The Department of Pediatrics, Washington University, St. Louis, MO

³The Division of Pediatric Infectious Diseases, Children's Hospital of Philadelphia, Philadelphia, PA

⁴The Department of Chemistry and Biochemistry, George Mason University, Fairfax, VA

KEYWORDS: MEP pathway, fosmidomycin, Dxr, malaria, tuberculosis, bisubstrate inhibitors

ABSTRACT. Tuberculosis and malaria are caused by the pathogens *Mycobacterium tuberculosis* (*Mtb*) and *Plasmodium falciparum* (*Pf*), respectively, and are two of the world's deadliest infectious diseases. These diseases' mortalities, complex life cycles of the causative agents, and the emergence of drug resistant strains highlight the necessity for novel treatments. Many modern antibiotics primarily target metabolic enzymes. As with most microbes, *Mtb* and *Pf* rely heavily on these enzymes to synthesize important secondary metabolites. Deoxy-D-xylulose-5-phosphate reductoisomerase (Dxr) has been identified as an essential enzyme because of its role in isoprenoid biosynthesis. Its importance in the methyl erythritol phosphate (MEP) pathway and presence in *Mtb* and *Pf*, but not in humans, distinguishes Dxr as a key target for inhibition. The natural products fosmidomycin and FR900098 are hydroxamate phosphonates that inhibit Dxr but exhibit poor pharmacokinetic properties and face challenges in cell permeability.¹ Based on these structures and prior inhibitors from our lab, we have designed and synthesized a novel series of small molecule, α,β -unsaturated FR900098 analogues with a variety of N-aroil substituents. Achieving considerable *in vitro* potency against whole cell *Pf* and the Dxr enzyme, we present the synthesis and biological evaluation of these compounds as therapeutic agents for malaria and tuberculosis.



■ INTRODUCTION

Malaria and tuberculosis are life-threatening diseases, which infect millions yearly. In 2017 alone, 219 million new malaria and 10 million new tuberculosis cases were reported, while there were 435,000 and 1.6 million deaths from each, respectively.¹ Drug resistance continues to prove itself as one of the largest challenges to contemporary therapeutic development, especially in the global effort to combat diseases prevalent in developing countries.² As these infectious microorganisms continually develop resistance to current drug therapies, it is essential to develop next-generation drugs to combat these threats.³ High rates of HIV coinfection further highlight the necessity of continued therapeutic development. Malaria and tuberculosis are also notoriously difficult to treat, though the mechanisms by which these resistances arise differ.

Malaria transmission occurs via a mosquito vector, where male and female haploids acquired from the blood of an infected individual reproduce inside the mosquito, after which new parasites are transferred to a non-infected individual by the insect.³ The mosquito takes in mature, blood-stage *Pf* parasites, releasing them into the bloodstream of the next individual upon feeding. The newly introduced parasites infect hepatocytes, where they multiply and mature until rupturing into the bloodstream. The parasites continue to mature in the bloodstream by invading erythrocytes, multiplying, and rupturing once more, surviving in the bloodstream at the cost of the host. These now-mature parasites may be taken up by another mosquito, which may go on to infect yet another

Received: August 16th, 2016

Published: May 17th, 2020

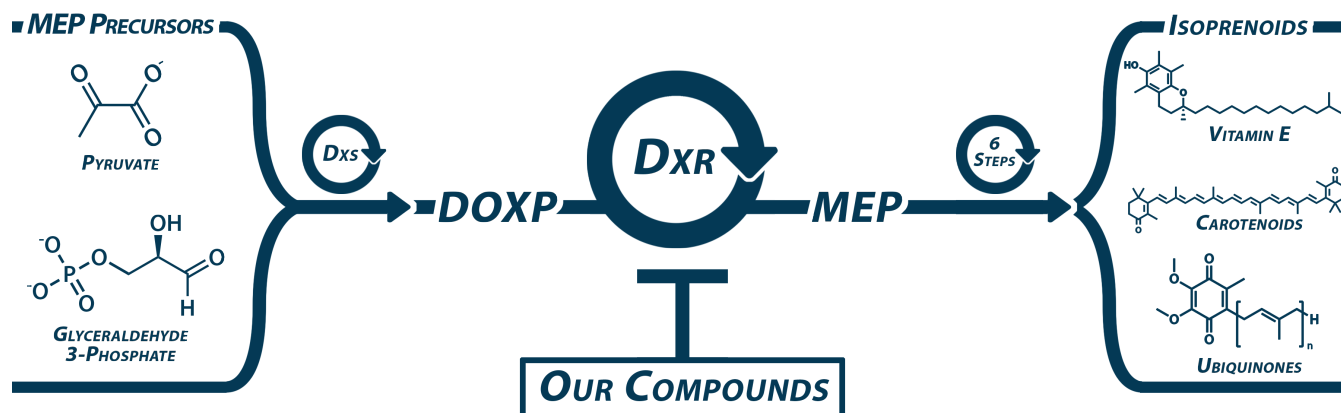


Figure 1. Illustrative inhibition of Dxr in the Methyl Erythritol Phosphate pathway.

individual.³ Overall, *Pf* has a complex lifecycle, including multiple stages both *in vivo* and *ex vivo*, with each stage reliant upon different enzymatic pathways for cell viability. This variability poses significant challenges to the treatment of pervasive malaria infections across communities.

The difficulties in treating tuberculosis arise not from a complex life cycle but rather from the pathological redundancies and frequent mutation of the *Mtb* bacterium itself. Tuberculosis occurs via the inhalation of *Mtb* bacteria, which, upon the failure of the host immune system to neutralize the invader, infect, multiply, and ultimately kill lung cells. Longstanding *Mtb* infections may expand throughout the body, causing acute system failure amongst other complications leading to host death.⁴ Though *Mtb* relies heavily on specific metabolic pathways that can be targeted with small molecules, its conservative mutagenesis and enzyme redundancy allow mutations to give rise to drug resistance quickly at no detriment to the viability nor virulence of the pathogen. Furthermore, latent *Mtb* infections are virtually impossible to clear, contributing significantly to the challenges faced in treating tuberculosis.⁵

Overall, the emergence of multi-drug resistant strains of these organisms highlights the importance of both effective antibiotics and versatile, efficient ways to prepare them. The pathogens behind these diseases develop resistance at an alarming rate, one which is unmatched by efforts to discover and synthesize small molecules in retaliation. The industrial neglect of these diseases and the increasing structural complexity of small molecule drugs facilitate this discrepancy, one which is projected to only worsen in the coming years.²

RESEARCH GOALS

Metabolic pathways are longstanding drug targets against human pathogens.⁶ The mevalonate pathway is one such target as it's necessary to maintain viability; though it is a demonstrably effective target, it is also present in humans, so its inhibition poses a cytotoxic risk.² Recently, however, the 2-C-methyl-D-erythritol 4-phosphate (MEP) pathway was

identified as a vital metabolic route for many pathogens.² Dxr (1-deoxy-D-xylulose-5-phosphate reductoisomerase) is an enzyme catalyzing the rate-limiting step of the MEP pathway, which provides the starting material for many important biomolecules. Not present in humans and the source for critical isoprenoids, the MEP pathway shows promise as a drug target.² Driven by these precepts, this project aims to develop small-molecule Dxr inhibitors to effectively combat MEP-metabolizing diseases (Figure 1).

Central to our approach are fosmidomycin and FR900098, natural products of bacterial origin that bind to Dxr but face pharmacokinetic challenges, such as cell permeability.⁴ Aiming to improve on the poor metabolic properties of fosmidomycin and to take advantage of additional binding interactions in the active and NADPH cofactor sites of Dxr, we sought to prepare a series of α,β -unsaturated, *N*-aroylated derivatives of this natural product. Early efforts showed that unsaturation of the carbon linker chain improved drug activity likely due to an increase in compound rigidity.^{8,9}

Dxr utilizes the common reductant NADPH to actuate its catalytic action on its natural substrate, DOXP. For this reaction to occur, DOXP must bind to Dxr's active site simultaneously to NADPH's nearby binding to the cofactor site.¹⁰ *N*-aroylation of fosmidomycin's retrohydroxamic acid achieves consecutive binding at both the active and cofactor sites, a technique known as bisubstrate inhibition.³ Taking advantage of additional binding interactions in this way may increase enzyme specificity and inhibitor potency. Seeking to probe the NADPH cofactor binding site in Dxr, we aim to explore a broad range of *N*-aroyl substitution patterns and to establish structure-activity relationships for these fosmidomycin analogues.

RESULTS AND DISCUSSION

Synthesis. *N*-aroyl analogues **GLB-49-55** and **RVB-56-61** were prepared as monosodium phosphonate salts in eight steps from commercially available starting materials shown in Scheme 1. *N*-aroyl analogues **GLB-107-123** were prepared in as diammonium phosphonate salts via the

same route. First, allyl diethyl phosphonate **1** was synthesized from triethylphosphite and allyl bromide via a neat Arbuzov reaction at 60 °C over two days in 83–87 % yield. Purification via Kugelrohr distillation and subsequent addition of bromine to the clear distillate in methylene chloride afforded dibromide compound **2**. *O*-benzylhydroxylamine hydrochloride was neutralized *in situ* via one stoichiometric equivalent of triethylamine in H₂O and methylene chloride at room temperature, after which di-*tert*-butyldicarbonate was added to yield Boc-protected intermediate **3**. Compounds **2** and **3** were reacted with two stoichiometric equivalents of sodium hydride in tetrahydrofuran to form compound **4**. The first equivalent of NaH deprotonated **3**, generating a nucleophile to attack and replace the γ -carbon bromide of **2**. The second equivalent of NaH deprotonated the α -carbon **2** to eliminate the β -bromide, installing the double bond and constructing **4**. Trifluoroacetic acid in methylene chloride was used to remove the protecting Boc group of **4**, generating the free hydroxylamine intermediate, which was aroylated via substituted benzoyl chlorides and sodium carbonate in methylene chloride to form *N*-aroyl intermediates **5a–w** in 24 hours at room temperature in 38–61% yields. Cleavage of the benzyl group using boron trichloride in methylene chloride afforded retrohydroxamic acids **6a–w** after reaction at –78 °C for two hours in 49–73% yields. Subjecting these retrohydroxamic acids to bromotrimethylsilane in methylene chloride and the subsequent addition of either sodium hydroxide in water or ammonia in methanol yielded monosodium or diammonium salts **7a–i** or **8a–i**, respectively, in >70% yields. As discussed later, monosodium salt compounds displayed instability, prompting the synthesis of diammonium salts in their places.

Biological Evaluation of *N*-aroyl, α,β -unsaturated Fosmidomycin Derivatives. In total, this project generated 16 unique compounds bearing *N*-aroyl substituents as α,β -unsaturated fosmidomycin derivatives. The first iteration of inhibitors was prepared as monosodium salts of the phosphonic acid, shown in Scheme 1; their inhibitory activities against whole cell *Pf* and Dxr are presented in Table 1. The *N*-aroyl substituents of these compounds were selected to encompass a range of electronic and steric properties to broadly explore the SAR around the aryl ring and further determine if we achieve bisubstrate inhibition. Only a handful of these compounds exhibited activities of higher potency than the previously prepared, unsubstituted *N*-benzoyl compound JXW-581, which is listed in Tables 1 and 2 for reference.

Though a common substituent trend is not definitive, higher activities are observed in compounds bearing *meta*- and *para*-electron-withdrawing moieties, as indicated by compounds RVB-57, GLB-55, GLB-53, GLB-49, and RVB-61. Utilizing an additional dipole–dipole binding interaction in the cofactor site

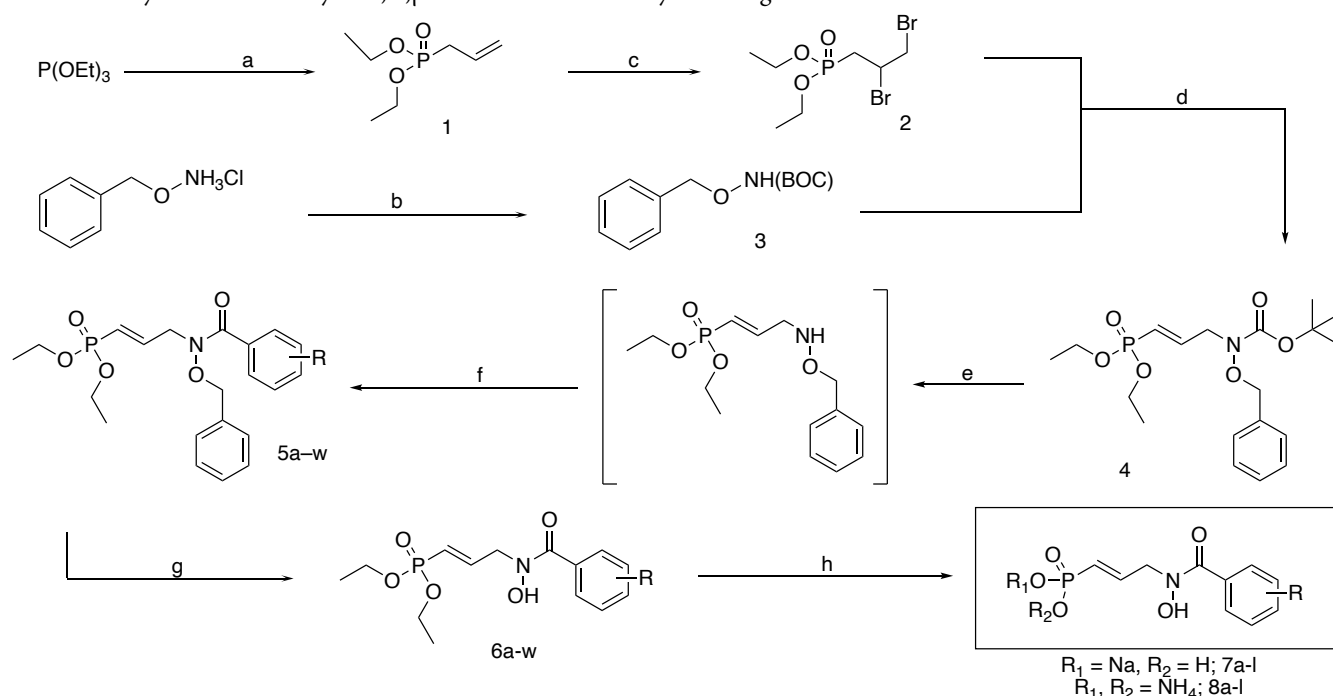
of Dxr may cause this increase in activity beyond that of the unsubstituted JXW-581. Contrarily, large lipophilic substituents caused drastic decreases in activity, possibly by preventing optimal binding via steric clash with cofactor site residues. The discrepancy in activity between the high *Pf* IC₅₀ and relatively low Dxr IC₅₀ values of the *N*-isonicotinoyl derivative, GLB-54, may be explained either by the poor solubility properties of the compound or the polarity of the *N*-pyridinyl substituent preventing cell permeation. This calls for further testing.

Table 1. Biological evaluation of the monosodium salt series against whole cell *Pf* and isolated Dxr. IC₅₀ values determined via PicoGreen fluorescence assay and are given in [μ M].

Cmpd	R ₁	<i>Pf</i> IC ₅₀	Dxr IC ₅₀
JXW-581	Ph	0.294	n.d.
RVB-57	(4-SMe)Ph	0.104	0.04136
GLB-53	(3-CF ₃)Ph	0.169	0.04800
GLB-55	(3,5-diCl)Ph	0.176	0.06432
GLB-49	(3-Cl)Ph	0.266	0.1580
RVB-61	(4-Cl)Ph	0.303	0.04400
GLB-51	2-naphthyl	1.208	0.4707
RVB-58	<i>p</i> -toluyl	1.300	0.1635
RVB-59	(4-CF ₃)Ph	2.499	0.1457
GLB-50	(4-Ph)Ph	4.378	0.2904
RVB-60	1-naphthyl	5.479	1.797
GLB-54	4-pyridinyl	6.525	0.5186
RVB-56	(4-F)Ph	20.215	n.d.
GLB-52	(4- <i>t</i> Bu)Ph	43.707	n.d.

Though the biological data from the first generation of *N*-aroyl substituents illustrated a rough outline of SAR, numerous challenges arose in both their preparation and testing. Some monosodium salt compounds exhibited extremely poor solubility across a range of solvents, causing challenges in accurate inhibitory data acquisition. Furthermore, the compound series displayed a propensity to hydrate upon prolonged suspension in dimethyl sulfoxide (as DMSO is exceedingly hygroscopic), an obvious concern for both testing and long-term storage. Indeed, nearly every batch of frozen DMSO stocks of the compounds listed in Table 1 saw this hydration.

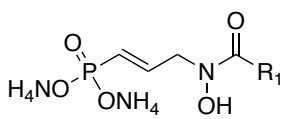
To address the aforementioned challenges, the first-generation compounds were prepared instead as diammonium salts via Scheme 1, as these salts have been shown to display

Scheme 1. Synthesis of *N*-Aroylated, α,β -unsaturated fosmidomycin analogues as diammonium or monosodium salts.^a

^aReagents and conditions: (a) allyl bromide, 60 °C, 2 days (83–87%); (b) (i) triethylamine, methylene chloride, water, rt, 30 min (ii) di-*tert*-butyldicarbonate, rt, 2 hours (95%); (c) bromine, methylene chloride, 0 °C, 1 hour (quant); (d) 2 eq NaH, THF, rt, 24 hours (70 %); (e) trifluoroacetic acid, methylene chloride, 0 °C, 1 hour (quant); (f) *R*-aroyl chloride, sodium carbonate, methylene chloride, 0 °C to rt, 24 hours (38–61%); (g) 1M boron trichloride in DCM, methylene chloride, –78 °C, 2 hours (49–73%); (h) (i) TMSBr, methylene chloride, 0 °C, 24 hours (ii) methanol, 1 hour (iii) NaOH, water, rt, 24 hours or (iii) 7N NH₃ in methanol, rt, 24 hours (>70%)

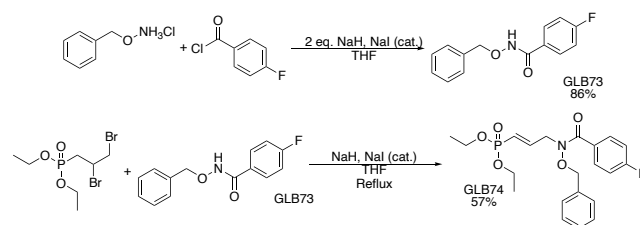
more favorable solubility properties and are generally easier to handle in solid form. Samples are being stored neat (undiluted) until testing to avoid hydration. Their inhibitory activities against whole cell *Pf* are presented in Table 2, and the *Pf* growth inhibition vs. drug concentration curves are shown in Figure 2.

Table 2. Biological evaluation data of diammonium salt series against whole cell *Pf* and isolated Dxr. IC₅₀ values determined via PicoGreen fluorescence assay and are given in [μM].

		
Cmpd	R ₁	<i>Pf</i> IC ₅₀
JXW-581	Ph	0.294
GLB-107	(4-SMe)Ph	13.46
GLB-106	(4-CF ₃)Ph	0.1579
GLB-119	(4-OMe)Ph	0.1624
GLB-102	(3-Cl)Ph	0.1990
GLB-122	(4-F)Ph	0.2540
GLB-105	(3,5-diCl)Ph	0.3304
GLB-103	(4-Cl)Ph	0.5735
GLB-120	(3,4-diCl)Ph	0.7003
GLB-121	(3-F)Ph	0.7218
GLB-123	4-pyridinyl	9.841

Condensed Synthesis via *N*-aroyl *O*-benzylhydroxylamines. The synthesis employed to prepare these compounds (shown in Scheme 1) sees concerns over the nucleophilicity of *N*-aroyl *O*-benzylhydroxylamines leading to the incorporation of a BOC protecting group to activate the amine prior to the coupling reaction. This necessitates the use of trifluoroacetic acid (TFA) to deprotect the newly formed intermediate to incorporate the aroyl moiety present in the target compounds.

Scheme 2. Alternative route to prepare *N*-benzoylated *O*-benzyl hydroxamate intermediates.



Some synthetic alternatives were explored in an effort to improve the efficiency of the synthesis currently employed. In particular, we sought to devise an alternate strategy to prepare the aryl hydroxamate–phosphonate coupled intermediates. These approaches explored the nucleophilicity of various *N*-substituted *O*-benzylhydroxylamines in the substitution of diethyl (2, 3-dibromopropyl) phosphonate. The most successful and promising of these attempts involves the *N*-

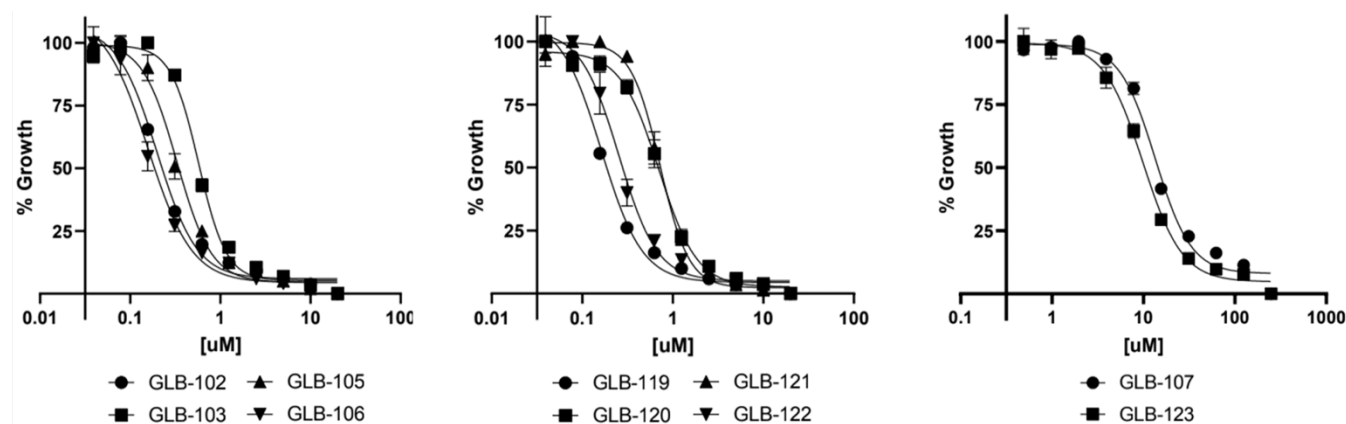


Figure 2. Growth inhibition curves of *Plasmodium falciparum* against μM concentration of diammonium salt analogues.

substitution of *O*-benzylhydroxylamine via nucleophilic attack of various *R*-benzoyl chlorides prior to adjoining the phosphonate and hydroxamate regions. Scheme 2 illustrates this reaction. Preparing the coupled *N*-benzoyl phosphonate intermediate in this alternative fashion eliminates the BOC protection step and, as such, removes the highly caustic TFA deprotection step altogether. Furthermore, this method achieves similar yields of the coupled intermediate and reduces time-to-target as substituted *N*-aroyl *O*-benzylhydroxylamines are largely crystalline^{11, 12} and may be prepared rapidly via Scheme 2.

CONCLUSIONS AND FUTURE DIRECTIONS

The preparation of this compound series marks a promising area of study for malaria and tuberculosis therapeutics. The development of modestly potent compounds effective against *Pf* Dxr compounds this promise. It may be of value to explore the effect of the linker length between the hydroxamate nitrogen and the aromatic moiety (Figure 3). Earlier studies showed the importance of the retrohydroxamic acid structure⁵; repositioning of the cofactor site-probing aryl group has been explored previously by our group,¹⁰ though not with the unsaturated backbone.

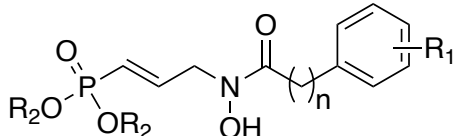


Figure 3. C_n linked analogues illustrated to explore adjacency of NADPH binding site in Dxr.

The compounds studied herein each bear C_0 linkers; projecting the aryl group further from the hydroxamate may allow for tighter binding to the NADPH cofactor site of Dxr simultaneous to active site binding by the western side of the molecule. Our previous work showed a 1.51-fold increase in potency from a C_1 linked to a C_3 linked *N*-phenyl fosmidomycin analogue.¹⁰ It is important to note that these two compounds

were still notably less potent than fosmidomycin's monosodium salt itself against *Pf* and were not α,β -unsaturated.

Though these Dxr inhibitors display considerable *in vitro* enzyme inhibition properties, the highly polar phosphonate moiety detrimental to fosmidomycin's therapeutic agency remains unaddressed. Both *Pf* and *Mtb* reside largely intracellularly during the duration of infection. Logically, any drug must readily pass through the membrane of an infected cell to affect its therapeutic action on the pathogen inside. Because cell membrane passage requires moving through the nonpolar interior of a phospholipid bilayer, polar molecules will be discouraged from entry. As such, *in vivo*, it is expected that each of these compounds will still face challenges in cell permeability, as the phosphonate region remains ionized at biological pH, thereby discouraging efficient cell membrane passage. Furthermore, the free phosphonate moiety is prone to metabolism via CYP450 monooxygenases, further limiting the bioavailability of the drug compound.¹³

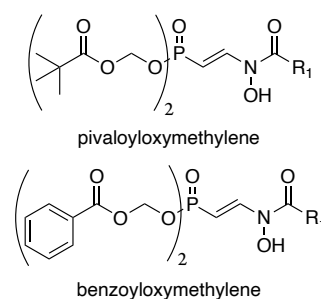


Figure 4. Bis-POM and Bis-BOM phosphonate prodrug derivatives of α,β -unsaturated, *N*-benzoylated fosmidomycin derivatives.

To address this challenge, lipophilic BOM (benzoyloxymethylene) and POM (pivaloyloxymethylene) groups will be coupled to the phosphonate moiety to form phosphonic esters as shown in Figure 4. These compounds are known as prodrugs, as the POM and BOM esters are cleaved *in vivo* via endogenous esterases to deploy the active phosphonate compound.¹⁴ Upon ester hydrolysis, the active compound is

deployed into the pathogen cell, resulting in an increase in bioaccumulation of the active drug at target sites, allowing the drug to affect its therapeutic potential.

Malaria and tuberculosis remain globally prevalent, deadly diseases. This compound series furthers the understanding of MEP pathway inhibition and the role of Dxr therein. Bisubstrate binding marks a promising method for enzyme inhibition, improving not only binding strength but also target specificity, and, as a result, metabolic resilience, as bisubstrate inhibitors are less likely to fit other enzymes. The techniques necessitated by the preparation of substituted retrohydroxamic acids and phosphonate esters find use in numerous other natural product syntheses, and their development contributes to innumerable disease therapies.

As Dxr isozymes are present in many infectious disease pathogen genomes, future studies could elucidate efficacious compounds against pathogenic bacteria responsible for other global disease challenges. Furthermore, access to structurally complex, diverse portions of chemical space are challenges faced not only in natural product derivatization but also in broader medicinal and synthetic chemistry. Though the various families of natural products, drug compounds, and therapeutic technologies we have discovered yet are significantly medically relevant, the sustained development of novel strategies for their preparation and modification are of equal importance.

■ EXPERIMENTAL

General. ^1H and ^{13}C NMR spectra were recorded in CDCl_3 , CD_3OD , or $(\text{CD}_3)_2\text{SO}$ on an Agilent spectrometer at 400 MHz with TMS as the internal standard. Chemical shifts are given in parts per million (ppm). Spin multiplicities are given with the following abbreviations: s (singlet), br s (broad singlet), d (doublet), dd (doublet of doublets), t (triplet), q (quadruplet), qt (quintuplet), m (multiplet). Thin layer chromatography (TLC) was performed on Baker-flex Silica Gel IB2-F silica plates. Flash chromatography was performed on a Biotage IsoleraTM One Flash Chromatography system. All reagents were purchased from commercial suppliers and used without further purification. Anhydrous solvents were purified by an MBRAUN MB-SPS solvent purification system before use. All air sensitive reactions were carried out under nitrogen or argon atmosphere.

Diethyl (prop-2-en-1-yl) phosphonate (1). Title compound was prepared following the method reported prior.¹

Diethyl(2,3-dibromopropyl) phosphonate (2). Title compound was prepared following the method reported prior.¹

tert-Butyl N-(benzyloxy) carbamate (3). Title compound was prepared following the method reported prior.¹

tert-butyl-N-(benzyloxy)-N-[(2E)-3-(diethoxyphosphoryl) prop-2-en-1-yl] carbamate (4). Title compound was prepared following the method reported prior.¹

General procedure A for synthesis of 5a-w (Boc deprotection and N-substitution). To a solution of **4** (1 eq, 1.00g, 2.506 mmol) in dry CH_2Cl_2 (0.6 M) at 0 °C under N_2 atmosphere was added trifluoroacetic acid (0.3 M) dropwise. The reaction mixtures were stirred overnight to room temperature, at which point complete conversion of **4** was observed by TLC in 1:1 CH_2Cl_2 :EtOAc. The reactions were quenched with saturated NaHCO_3 (aq., 50 mL) and extracted with CH_2Cl_2 (3 \times 50 mL). The combined organic layers were washed with saturated NaCl (aq., 20 mL), dried over anhydrous Na_2SO_4 , filtered, and concentrated under reduced pressure. The crude concentrate was pre-incubated for 5 minutes in dry CH_2Cl_2 (0.3 M) under N_2 atmosphere with Na_2CO_3 (5 eq). Aroyl chlorides (2 eq) were added dropwise to the reaction mixture at 0 °C, which was allowed to stir overnight. The reaction was quenched with saturated NaHCO_3 (aq., 50 mL) and extracted with CH_2Cl_2 (3 \times 50 mL). The combined organic layers were washed with saturated NaCl (aq., 20 mL), dried over anhydrous Na_2SO_4 , filtered, and concentrated under reduced pressure. Chromatographic separation of the crude concentrate on silica gel (CH_2Cl_2 /EtOAc = 1/0 to 3/2) gave the title compounds as yellow oils in yields ranging from 38–61%.

General procedure B for synthesis of 6a-w (O-Debenzylation). To a solution of one of **5a-w** (1 eq) in dry CH_2Cl_2 (0.3 M) at -78 °C under N_2 atmosphere was added boron trichloride (1M solution in CH_2Cl_2 , 5 eq) dropwise. The reaction mixtures were allowed to stir for 1-2 hours at -78 °C and were monitored by TLC in EtOAc and LCMS. The reactions were quenched with saturated NaHCO_3 (aq., 50 mL) and extracted with CH_2Cl_2 (3 \times 50 mL) and EtOAc (1 \times 50 mL). The combined organic layers were washed with saturated NaCl (aq., 20 mL), dried over anhydrous Na_2SO_4 , filtered, and concentrated under reduced pressure. Chromatographic separation of the crude concentrate on silica gel (EtOAc) or via flash chromatography (EtOAc/MeOH = 1/0 to 10/1) gave the title compounds as pale yellow oils or pale-yellow crystalline solids in yields ranging from 49–73%.

General procedure C for synthesis of 7a-l (Phosphonate transesterification and monosodium ion pairing). To a solution of one of **6a-l** (1 eq) in dry CH_2Cl_2 (0.25 M) at 0 °C under N_2 atmosphere was added bromotrimethylsilane dropwise. The reaction mixtures were allowed to stir for 24 hours at ambient temperature and were monitored by TLC in EtOAc and by LCMS. The reactions were quenched via serial dilution with CH_2Cl_2 and concentration under reduced pressure. To a solution of the crude concentrates in water at room temperature was added aqueous NaOH (1.05 eq). The reaction mixtures were allowed to stir for 24 hours at ambient temperature. Concentration under reduced pressure and subsequent lyophilization gave the title compounds as pale

yellow or orange crystalline solids in yields ranging from 65–88%.

General procedure D for synthesis of 8a-1 (Phosphonate transesterification and diammonium ion pairing). To a solution of one of **6m-w** (1 eq) in dry CH_2Cl_2 (0.25 M) at 0°C under N_2 atmosphere was added bromotrimethylsilane dropwise. The reaction mixtures were allowed to stir for 24 hours at ambient temperature and were monitored by TLC in EtOAc and by LCMS. The reactions were quenched via serial dilution with CH_2Cl_2 and concentration under reduced pressure. To a solution of the crude concentrates in dry MeOH at room temperature under N_2 atmosphere was added 7N NH_3 in MeOH (2 eq) dropwise. The reaction mixtures were allowed to stir for 24 hours at ambient temperature. Concentration under reduced pressure and subsequent lyophilization gave the title compounds as pale yellow or orange crystalline solids in yields ranging from 76–92%.

■ SPECTROSCOPIC DATA

GLB-49 (Sodium hydrogen $[(1E)-3-[1-(3\text{-chlorophenyl})-N\text{-hydroxyformamido}] \text{prop-1-en-1-yl}]$ phosphonate). ^1H NMR (400 MHz, cd_3od) δ 7.96 – 7.28 (m, 5H), 6.54 – 6.24 (m, 1H), 6.07 (ddq, $J = 17.4$, 16.1, 1.6 Hz, 1H), 4.97 – 4.82 (m, 9H), 4.38 (s, 1H), 3.35 – 3.21 (m, 2H).

GLB-50 (Sodium hydrogen $[(1E)-3-(1-[1,1'\text{-biphenyl-4-yl}]-N\text{-hydroxyformamido}) \text{prop-1-en-1-yl}]$ phosphonate). ^1H NMR (400 MHz, cd_3od) δ 8.12 – 7.99 (m, 1H), 7.79 – 7.48 (m, 7H), 7.48 – 7.22 (m, 4H), 6.58 – 6.35 (m, 1H), 6.28 – 6.00 (m, 1H), 4.41 (s, 1H), 3.34 (s, 1H), 1.26 (s, 1H).

GLB-51 (Sodium hydrogen $[(1E)-3-[N\text{-hydroxy-1-(naphthalen-2-yl)formamido}] \text{prop-1-en-1-yl}]$ phosphonate). ^1H NMR (400 MHz, cd_3od) δ 7.37 – 7.17 (m, 1H), 6.81 – 6.55 (m, 7H), 6.41 – 6.18 (m, 4H), 5.42 – 5.08 (m, 1H), 5.08 – 4.68 (m, 1H), 3.62 (s, 19H), 3.19 (s, 1H), 2.09 – 1.94 (m, 2H).

GLB-52 (Sodium hydrogen $[(1E)-3-[1-(4\text{-tert-butylchlorophenyl})-N\text{-hydroxyformamido}] \text{prop-1-en-1-yl}]$ phosphonate). ^1H NMR (400 MHz, cd_3od) δ 7.95 – 7.84 (m, 3H), 7.80 – 7.58 (m, 1H), 7.49 – 7.36 (m, 7H), 6.33 (dt, $J = 17.3$, 5.4 Hz, 1H), 6.03 (q, $J = 17.5$, 15.9 Hz, 1H), 5.09 (d, $J = 2.4$ Hz, 2H), 4.10 (d, $J = 4.7$ Hz, 1H), 1.34 (s, 13H).

GLB-53 (Sodium hydrogen $[(1E)-3-[1-(3\text{-trifluoromethylphenyl})-N\text{-hydroxyformamido}] \text{prop-1-en-1-yl}]$ phosphonate). ^1H NMR (400 MHz, dmso) δ 8.23 – 7.52 (m, 6H), 6.30 (d, $J = 17.8$ Hz, 1H), 5.92 (t, $J = 16.4$

Hz, 1H), 4.40 – 4.24 (m, 4H), 3.18 (s, 1H), 1.33 – 1.13 (m, 1H).

GLB-54 (Sodium hydrogen $[(1E)-3-[N\text{-hydroxy-1-(pyridin-4-yl)formamido}] \text{prop-1-en-1-yl}]$ phosphonate). ^1H NMR (400 MHz, dmso) δ 8.76 (dd, $J = 31.7$, 5.1 Hz, 1H), 7.98 – 7.51 (m, 1H), 6.54 – 6.29 (m, 1H), 5.95 (t, $J = 17.7$ Hz, 1H), 4.43 (s, 1H), 1.38 – 1.05 (m, 1H).

GLB-55 (Sodium hydrogen $[(1E)-3-[1-(3,5\text{-dichlorophenyl})-N\text{-hydroxyformamido}] \text{prop-1-en-1-yl}]$ phosphonate). ^1H NMR (400 MHz, cd_3od) δ 7.71 – 6.92 (m, 4H), 6.20 (dddd, $J = 19.3$, 17.0, 7.6, 5.6, 2.3 Hz, 1H), 5.84 (t, $J = 16.7$ Hz, 1H), 4.38 – 4.02 (m, 2H), 1.06 (d, $J = 8.7$ Hz, 1H).

RVB-56 (Sodium hydrogen $[(1E)-3-[1-(4\text{-fluorophenyl})-N\text{-hydroxyformamido}] \text{prop-1-en-1-yl}]$ phosphonate). ^1H NMR (400 MHz, Methanol- d_4) δ 7.67 (s, 2H), 7.16–7.01 (m, 2H), 6.42–6.18 (m, 1H), 6.15–5.92 (m, 1H), 4.28 (s, 2H).

RVB-57 (Sodium hydrogen $[(1E)-3-[N\text{-hydroxy-1-[4-(methylsulfanyl)phenyl]formamido}] \text{prop-1-en-1-yl}]$ phosphonate). ^1H NMR (400 MHz, Methanol- d_4) δ 7.93–7.81 (m, 1H), 7.66–7.55 (m, 1H), 7.27–7.20 (m, 2H), 6.53–6.36 (m, 1H), 6.18–5.99 (m, 1H), 4.36 (d, $J = 5.6$ Hz, 2H), 2.53–2.43 (m, 3H).

RVB-58 (Sodium hydrogen $[(1E)-3-[1-(4\text{-methylphenyl})-N\text{-hydroxyformamido}] \text{prop-1-en-1-yl}]$ phosphonate). ^1H NMR (400 MHz, DMSO- d_6) δ 7.77 (d, $J = 21.2$ Hz, 1H), 7.58 (s, 1H), 7.13 (s, 2H), 6.47–6.09 (m, 1H), 6.09–5.76 (m, 1H), 4.57–3.86 (m, 2H), 2.28 (s, 3H).

RVB-59 (Sodium hydrogen $[(1E)-3-[1-(4\text{-trifluoromethylphenyl})-N\text{-hydroxyformamido}] \text{prop-1-en-1-yl}]$ phosphonate). ^1H NMR (400 MHz, Methanol- d_4) δ 8.18–7.75 (m, 2H), 7.69 (d, $J = 30.7$ Hz, 2H), 6.49 (q, $J = 22.2$, 18.8 Hz, 1H), 6.07 (t, $J = 17.3$ Hz, 1H), 4.44 (s, 2H).

RVB-60 (Sodium hydrogen $[(1E)-3-[N\text{-hydroxy-1-(naphthalen-2-yl)formamido}] \text{prop-1-en-1-yl}]$ phosphonate). ^1H NMR (400 MHz, Methanol- d_4) δ 8.18–7.75 (m, 2H), 7.69 (d, $J = 30.7$ Hz, 2H), 6.49 (q, $J = 22.2$, 18.8 Hz, 1H), 6.07 (t, $J = 17.3$ Hz, 1H), 4.44 (s, 2H).

RVB-61 (Sodium hydrogen $[(1E)-3-[1-(4\text{-chlorophenyl})-N\text{-hydroxyformamido}] \text{prop-1-en-1-yl}]$ phosphonate). ^1H NMR (400 MHz, Methanol- d_4) δ 7.71 (d, $J = 97.1$ Hz, 2H), 7.27 (d, $J = 16.9$ Hz, 2H), 6.60–6.19 (m, 1H), 6.22 – 5.86 (m, 1H), 4.543.70 (m, 2H).

GLB-102 (Diammonium $[(1E)-3-[1-(3\text{-chlorophenyl})-N\text{-hydroxyformamido}] \text{prop-1-en-1-yl}]$ phosphonate). ^1H

NMR (400 MHz, dmso) δ 7.92 – 7.28 (m, 4H), 6.20 (s, 1H), 5.81 (t, J = 16.1 Hz, 1H), 4.23 (s, 2H), 3.84 (s, 1H), 2.66 – 2.44 (m, 8H). HRMS (ESI⁺) calculated for C₁₀H₁₂ClNO₅P 292.0136, found 292.0138 [M+H].

GLB-103 (Diammonium [(1E)-3-[1-(4-chlorophenyl)-N-hydroxyformamido]prop-1-en-1-yl] phosphonate). ¹H NMR (400 MHz, dmso) δ 7.99 – 7.33 (m, 4H), 6.21 (t, J = 18.2 Hz, 1H), 5.82 (t, J = 16.2 Hz, 1H), 4.24 (s, 2H), 3.84 (s, 1H), 3.14 (d, J = 1.1 Hz, 1H). HRMS (ESI⁺) calculated for C₁₀H₁₂ClNO₅P 292.0136, found 292.0136 [M+H].

GLB-105 (Diammonium [(1E)-3-[1-(3,5-dichlorophenyl)-N-hydroxyformamido]prop-1-en-1-yl] phosphonate). ¹H NMR (400 MHz, dmso) δ 7.88 – 7.62 (m, 4H), 6.22 (s, 1H), 5.83 (t, J = 16.2 Hz, 1H), 4.24 (s, 2H), 3.86 (d, J = 0.7 Hz, 1H), 3.14 (s, 1H). HRMS (ESI⁺) calculated for C₁₀H₁₁Cl₂NO₅P 325.9749, found 325.9740 [M+H].

GLB-106 (Diammonium [(1E)-3-[1-(4-trifluoromethylphenyl)-N-hydroxyformamido]prop-1-en-1-yl] phosphonate). ¹H NMR (400 MHz, dmso) δ 8.07 – 7.51 (m, 3H), 6.24 (s, 1H), 5.84 (t, J = 16.1 Hz, 1H), 4.27 (d, J = 5.4 Hz, 2H), 3.14 (d, J = 1.0 Hz, 3H). HRMS (ESI⁺) calculated for C₁₁H₁₂F₃NO₅P 326.0400, found 326.0401 [M+H].

GLB-107 (Diammonium [(1E)-3-[N-hydroxy-1-[4-(methylsulfanyl)phenyl]formamido]prop-1-en-1-yl] phosphonate). ¹H NMR (400 MHz, dmso) δ 7.87 – 7.60 (m, 2H), 7.31 – 7.18 (m, 2H), 6.21 (t, J = 18.0 Hz, 1H), 5.88 – 5.68 (m, 1H), 4.22 (s, 1H), 1.33 – 1.15 (m, 3H), 0.91 – 0.73 (m, 1H). HRMS (ESI⁺) calculated for C₁₁H₁₅NO₅PS 304.0403, found 304.0402 [M+H].

GLB-119 (Diammonium [(1E)-3-[N-hydroxy-1-(4-methoxyphenyl)formamido]prop-1-en-1-yl] phosphonate). ¹H NMR (400 MHz, DMSO-d₆) δ . HRMS (ESI⁺) calculated for C₁₁H₁₅NO₆P 288.0632, found 288.0634 [M+H].

GLB-120 (Diammonium [(1E)-3-[N-hydroxy-1-(3,4-dichlorophenyl)formamido]prop-1-en-1-yl] phosphonate). ¹H NMR (400 MHz, dmso) δ 7.07 – 6.78 (m, 2H), 6.23 – 5.98 (m, 2H), 5.36 (t, J = 17.8 Hz, 1H), 5.05 – 4.85 (m, 1H), 3.37 (s, 2H), 3.06 – 2.85 (m, 3H), 0.38 (s, 1H). HRMS (ESI⁺) calculated for C₁₀H₁₁Cl₂NO₅P 325.9747, found 325.9745 [M+H].

GLB-121 (Diammonium [(1E)-3-[N-hydroxy-1-(3-fluorophenyl)formamido]prop-1-en-1-yl] phosphonate). ¹H NMR (400 MHz, dmso) δ 7.76 – 7.60 (m, 1H), 7.53 – 7.33 (m, 3H), 7.30 – 7.16 (m, 1H), 6.21 (t, J = 18.1 Hz, 1H), 5.84 (t, J = 16.2 Hz, 1H), 4.25 (s, 2H), 3.13 (d, J =

0.7 Hz, 1H), 1.21 (s, 1H). HRMS (ESI⁺) calculated for C₁₀H₁₂FNO₅P 276.0432, found 276.0435 [M+H].

GLB-122 (Diammonium [(1E)-3-[N-hydroxy-1-(4-fluorophenyl)formamido]prop-1-en-1-yl] phosphonate). ¹H NMR (400 MHz, dmso) δ 8.00 – 7.86 (m, 1H), 7.76 (d, J = 8.1 Hz, 1H), 7.30 – 7.08 (m, 2H), 6.19 (d, J = 18.4 Hz, 1H), 5.90 – 5.69 (m, 1H), 4.24 (s, 1H), 2.45 (s, 6H), 1.23 (d, J = 17.3 Hz, 1H). HRMS (ESI⁺) calculated for C₁₀H₁₂FNO₅P 276.0432, found 276.0433 [M+H].

GLB-123 (Diammonium [(1E)-3-[N-hydroxy-1-(pyridin-4-yl)formamido]prop-1-en-1-yl] phosphonate). ¹H NMR (400 MHz, DMSO-d₆) δ . HRMS (ESI⁺) calculated for C₉H₁₂N₂O₅P 259.0479, found 259.0481 [M+H].

AUTHOR INFORMATION

Corresponding Author

*Email: logan_bartholomew@berkeley.edu

Author Contributions

The manuscript was written by the leading author and valuable revisions were given by KMH and CSD.

Funding Sources

Funds were provided by the Department of Chemistry at The George Washington University and the National Institutes of Health.

ACKNOWLEDGEMENT

This work represents the culmination of my undergraduate career. For the opportunities, knowledge, skills, and insights I have been fortunate to accrue, I cannot thank (soon to be Dr.) Kenny Heide and Dr. Cindy Dowd enough for their combined invaluable mentorship and impressive tolerance of my frequent incompetence. I will always cherish my time in the Dowd group, and I'm excited to bring along our tasteful sentiments to the University of California, Berkeley in the fall.

ABBREVIATIONS USED

DOXP, 1-deoxy-D-xylulose 5-phosphate; MEP; methyl erythritol phosphate; DCM, dichloromethane; EtOAc, ethyl acetate; Pf, *Plasmodium falciparum*; Mtb, *Mycobacterium tuberculosis*; Dxr, 1-deoxy-D-xylulose phosphate reductoisomerase; TMSBr, trimethylsilyl bromide; BCl₃, boron trichloride; NADPH, nicotinamide adenine dinucleotide phosphate hydride; SAR, structure-activity relationships; TFA, trifluoroacetic acid; BOC, butyl oxy carbonyl.

■ REFERENCES

- (1) Wang, Xu, Rachel L. Edwards, Haley Ball, Claire Johnson, Amanda Haymond, Misgina Girma, Michelle Manikkam et al. "MEPicides: α , β -unsaturated Fosmidomycin analogues as DXR inhibitors against malaria." *Journal of medicinal chemistry* 61, no. 19 (2018): 8847-8858.
- (2) Projan, Steven J. "Why is big Pharma getting out of antibacterial drug discovery?" *Current opinion in microbiology* 6, no. 5 (2003): 427-430.
- (3) Baum, Jake, Tim-Wolf Gilberger, Freddy Frischknecht, and Markus Meissner. "Host-cell invasion by malaria parasites: insights from Plasmodium and Toxoplasma." *Trends in parasitology* 24, no. 12 (2008): 557-563.
- (4) Centers for Disease Control (US), Center for Prevention Services (US). Division of Tuberculosis Elimination, and American Thoracic Society. *Core curriculum on tuberculosis*. US Department of Health & Human Services, Public Health Service, Centers for Disease Control, 1992.
- (5) Program, Tuberculosis Drug Screening. "Search for new drugs for treatment of tuberculosis." *Antimicrobial agents and chemotherapy* 45, no. 7 (2001): 1943.
- (6) Anishetty, Sharmila, Mrudula Pulimi, and Gautam Pennathur. "Potential drug targets in Mycobacterium tuberculosis through metabolic pathway analysis." *Computational biology and chemistry* 29, no. 5 (2005): 368-378.
- (7) R Jackson, Emily, and Cynthia S Dowd. "Inhibition of 1-deoxy-D-xylulose-5-phosphate reductoisomerase (Dxr): a review of the synthesis and biological evaluation of recent inhibitors." *Current topics in medicinal chemistry* 12, no. 7 (2012): 706-728.
- (8) Mac Sweeney, Aengus, Roland Lange, Roberta PM Fernandes, Henk Schulz, Glenn E. Dale, Alice Douangamath, Philip J. Proteau, and Christian Oefner. "The crystal structure of E. coli 1-deoxy-D-xylulose-5-phosphate reductoisomerase in a ternary complex with the antimalarial compound fosmidomycin and NADPH reveals a tight-binding closed enzyme conformation." *Journal of molecular biology* 345, no. 1 (2005): 115-127.
- (9) Uh, Eugene, Emily R. Jackson, Géraldine San Jose, Marcus Maddox, Robin E. Lee, Richard E. Lee, Helena I. Boshoff, and Cynthia S. Dowd. "Antibacterial and antitubercular activity of fosmidomycin, FR900098, and their lipophilic analogs." *Bioorganic & medicinal chemistry letters* 21, no. 23 (2011): 6973-6976.break
- (10) San Jose, Géraldine, Emily R. Jackson, Eugene Uh, Chinchu Johny, Amanda Haymond, Lindsay Lundberg, Chelsea Pinkham et al. "Design of potential bisubstrate inhibitors against Mycobacterium tuberculosis (Mtb) 1-deoxy-D-xylulose 5-phosphate reductoisomerase (Dxr)—evidence of a novel binding mode." *MedChemComm* 4, no. 7 (2013): 1099-1104.
- (11) Palakurthy, Nani Babu, Dharm Dev, Sonali Paikaray, Susmitnarayan Chaudhury, and Bhubaneswar Mandal. "Synthesis of O-benzyl hydroxamates employing the sulfonate esters of N-hydroxybenzotriazole." *RSC Advances* 4, no. 16 (2014): 7952-7958.
- (12) Gissot, Arnaud, Alessandro Volonterio, and Matteo Zanda. "One-step synthesis of O-benzyl hydroxamates from unactivated aliphatic and aromatic esters." *The Journal of organic chemistry* 70, no. 17 (2005): 6925-6928.
- (13) Tsuchiya, T., K. Ishibashi, M. Terakawa, M. Nishiyama, N. Itoh, and H. Noguchi. "Pharmacokinetics and metabolism of fosmidomycin, a new phosphonic acid, in rats and dogs." *European journal of drug metabolism and pharmacokinetics* 7, no. 1 (1982): 59-64.
- (14) Heidel, Kenneth M., and Cynthia S. Dowd. "Phosphonate prodrugs: an overview and recent advances." *Future medicinal chemistry* 11, no. 13 (2019): 1625-1643.